

ULTRA WIDEBAND RADAR SYSTEM FOR BLADDER MONITORING APPLICATIONS

M. O'Halloran^{1, *}, F. Morgan¹, D. Flores-Tapia², D. Byrne¹, M. Glavin¹, and E. Jones¹

¹College of Engineering and Informatics, National University of Ireland Galway, University Road, Galway, Ireland

²Division of Medical Physics, CancerCare Manitoba, Winnipeg, Manitoba R3E 0V9, Canada

Abstract—The aim of this study is to address the management of urinary problems by detecting changes in the volume of urine within the human bladder using low cost, low power, wearable Ultra Wideband (UWB) sensors and signal processing techniques. The paper describes experiments on the classification of six three-layer dielectrically representative bladder phantoms, mimicking a range of muscle and bladder wall-to-wall distances. The process involves the illumination of the bladder with a UWB pulse. Due to the dielectric contrast between urine and bladder wall tissue at microwave frequencies, an electromagnetic reflection is generated at both the anterior and posterior bladder wall. These reflections are recorded, the salient features are extracted and processed by a classification algorithm to estimate the volume of urine present in the bladder. To evaluate the prototype system, a number of physical bladder phantoms were constructed, each mimicking bladders of different volumes. Principal Component Analysis (PCA) was applied and the processed features were classified by a K -Nearest Neighbour learning algorithm to estimate the state of the bladder (small, medium or full). The paper describes the bladder phantom prototype systems and the experimental setup. Results illustrate detection of phantom bladder states with an accuracy of up to 91%.

1. INTRODUCTION

Bladder control problems include urinary incontinence, urinary retention and nocturnal enuresis (bed-wetting). Incontinence affects

Received 8 August 2012, Accepted 17 September 2012, Scheduled 26 September 2012

* Corresponding author: Martin O'Halloran (martin.ohalloran@gmail.com).

up 35% of people over the age of 60, amounting to over 200 million people worldwide [1]. Urinary incontinence is defined as the inability to stop the flow of urine from the bladder. Frequent urination or urgency to void the bladder can increase the risk of falls by 26% and bone fracture by as much as 34% [2]. Up to 50% of homebound and nursing home residents are incontinent, with an estimated societal cost of 12.6 billion dollars in the US annually [3].

Urinary retention is defined as the inability to urinate and can be caused by an obstruction in the urinary tract or by nerve problems that interfere with signals between the brain and the bladder. Urinary retention can be caused by childbirth, diabetes, stroke, spinal cord injuries, prostate enlargement, urinary tract infections (UTI), bladder stones, and surgery (due to anaesthetics). Urinary retention is generally treated by catheterization. Almost 10% of all men over the age of 70 and 33% of all men over the age of 80 will suffer from urinary retention at least once over a five year period [4]. Urinary retention can significantly increase the risk of kidney damage and urinary tract infections.

Finally, while incontinence and retention largely affects older people, enuresis (involuntary bed-wetting) is normally confined to children, and affects 5–7 million children in the US each year [5]. Enuresis is defined as involuntary urination, which can be caused by a variety of factors including disorders of the kidneys, bladder, or ureter; and poor control of the muscles that control release of urine. For the majority of children, there is no single explanation, either physical or psychological, for bedwetting.

Each of these conditions (and many other bladder-related medical conditions) could greatly benefit from a system that could monitor the bladder. While ultrasound-based solutions have been proposed [6, 7], such systems can often be limited by size, battery power consumption and cost. Therefore, an opportunity exists for an alternative bladder-state sensing system, based on Ultra Wideband (UWB) Radar.

Measuring water accumulation in the bladder using UWB Radar was previously investigated by Pancera et al. [8–10]. However, rather than attempting to estimate the exact bladder depth (and corresponding volume) using range-gating algorithms as investigated by Pancera et al., this study aims to classify the state of the bladder as either “Small”, “Medium” or “Full” using corresponding bladder phantoms with varying volumes of urine. The authors believe that this approach could be more robust to natural between-patient variations in skin, fat and muscle thicknesses and bladder sizes. A prototype system is presented in this paper and is evaluated on dielectrically representative bladder phantoms.

The remainder of the paper is organized as follows: The construction of the bladder phantoms and the prototype system is outlined in Section 2; Section 3 describes the bladder state classification algorithm, including signal pre-processing, feature extraction and a brief overview of the classification algorithm; Results are presented in Section 4, with a number of test scenarios to examine the robustness of the classification algorithm and finally, conclusions are drawn in Section 5.

2. BLADDER PHANTOMS & EXPERIMENTAL SETUP

In this section, the bladder phantoms and the experimental setup used to transmit and record the UWB signals are described.

2.1. Bladder Phantoms

In this study, several bladder phantoms were created, modeled as three-layer structures. The first and third layer contain tissue-mimicking material with dielectric properties similar to those of human muscle. The middle layer contained a saline solution, with similar dielectric properties to urine. The muscle-mimicking material was created using a 6.5:1 TX151 to water mixture, while the urine was represented by a 0.5% saline solution [9]. The dielectric properties of the muscle-mimicking material are described in Table 1. The various layers were separated by thin sheets of acrylic.

Two separate sets of phantoms were created, labeled Set I and Set II, corresponding to different muscle depths and bladder volumes. Set I phantoms had 10 mm muscle layers with bladder depths (distance between anterior and posterior muscle layer) measuring 10 mm (Small), 20 mm (Medium) and 30 mm (Full). Set II phantoms were more challenging from a UWB probing perspective, with 25 mm muscle layers and bladder depths measuring 20 mm (Small), 30 mm (Medium) and 40 mm (Full). An example of the phantom construction is shown in Figure 1.

Table 1. Complex permittivity of muscle-mimicking material.

Frequency MHz	Complex Permittivity
500	$78.45 - j19.55$
1000	$50.55 - j14.25$
2000	$34.7 - j10.05$
5000	$16.75 - j5.65$
10000	$7 - j3.1$



Figure 1. Diagram of the bladder phantom. The muscle depth is 10 mm for Set I and 25 mm for Set II.

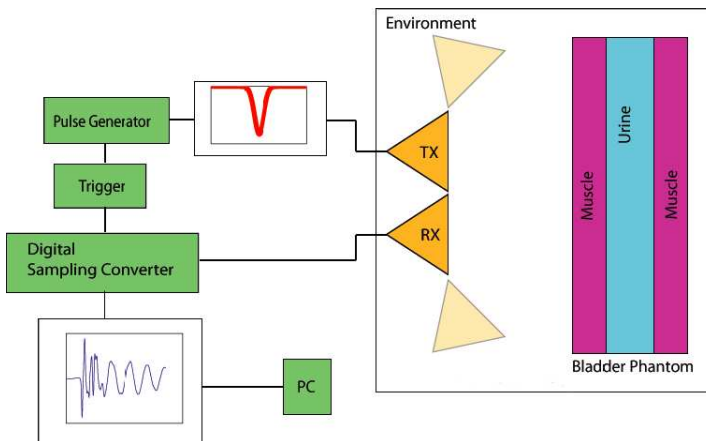


Figure 2. Block diagram of the UWB bladder system setup. The transmitting and receiving antennas are marked as “TX” and “RX” in the image.

2.2. Experimental Setup

A block diagram illustrating the UWB experimental setup is shown in Figure 2.

A GZ1118ANE pulse generator from *Geozondas* [11] was used to generate a monocycle pulse with a Full-Width Half-Maximum span of 220 ps. The mean transmitted power of the pulse generator was 1.6 mW. A bistatic antenna array was used to transmit and receive the UWB signals. Each antenna was a 2 Bow-tie Phased-array antenna with reflector of dimensions $113 \times 123 \times 57$ mm. The frequency-range of the antenna was 1–4.5 GHz.

The UWB pulse radiated from the transmitting element (TX)

into the phantom and the reflections are recorded at the receiver (RX). To synthesise a four element antenna array, four transmitting antenna positions are used, where three receiver locations collect the backscatter for each transmitter location. Each of these antenna locations is shown in Figure 2.

Twelve (4 TX \times 3 RX) transmitter/receiver combinations are used to acquire signal data at a specific perpendicular distance from the phantom. In order to introduce variance (to adequately test the bladder volume classifier), this distance between the antenna array and phantom is varied from 200 mm to 236 mm, in 3 mm increments during signal acquisition. A total of 60 (5 \times 12) signals are recorded for each phantom from Set I and Set II.

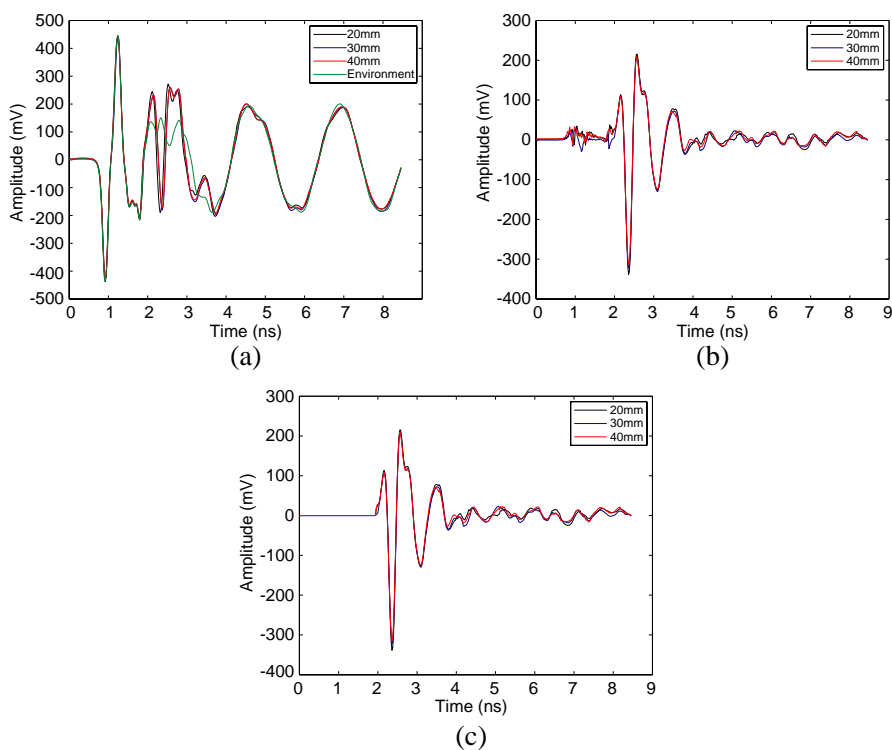


Figure 3. (a) All recorded signals. (b) All recorded signals after environment signal has been subtracted. (c) All signals after noise prior to first muscle wall reflection is removed.

3. BLADDER STATE CLASSIFICATION ALGORITHM

In this section, the bladder state classification algorithm is detailed, including the data pre-processing, feature extraction method and a brief overview of the k -nearest neighbour (kNN) classifier used.

3.1. Data Preprocessing

In order to remove unwanted background reflections and antenna coupling, measurements are first recorded without the phantom present. The resultant reference signals are then subtracted from all phantom signals before further processing. To further reduce noise, all signals prior to the dominant reflection (the first reflection from the anterior muscle wall) are set equal to zero, as shown in Figure 3.

3.2. Feature Extraction

In order to extract the most salient features of the UWB backscattered signals, Principal Component Analysis (PCA) is applied to the entire dataset [12]. PCA is used to reduce the dimensionality of the data and diminishes the influence of less relevant information such as noise [13]. A new orthonormal basis is derived which presents the dataset in terms of its variance. Components are listed in order of decreasing variance.

3.3. K Nearest Neighbour Learning Algorithm

The k Nearest Neighbour (kNN) learning algorithm is an example-based classifier where test features are classified by a majority vote of its k nearest neighbours in the feature space [14]. Given a training set of sample-label pairs (\mathbf{x}_i, y_i) , with features \mathbf{x}_i , labels y_i and $i = 1, \dots, M$, an attempt is made to classify an unknown sample \mathbf{q} by calculating its weighted distance from \mathbf{x}_i as:

$$d(\mathbf{q}, \mathbf{x}_i) = \sum_{j=1}^N w_j |\mathbf{q}_j - \mathbf{x}_{ij}| \quad (1)$$

To determine the class of \mathbf{q} , a majority distance weighted voting system is used where:

$$Vote(y_i) = \sum_{c=1}^k \frac{1}{|\mathbf{q} - \mathbf{x}_c|} 1(y_i, y_c) \quad (2)$$

where $1(y_i, y_c)$ returns 1 if the class labels match and 0 otherwise.

4. RESULTS

Prior to kNN classification, 180 signals for each set are shuffled 21 times and split into a testing and training set in the ratio of 1 : 3 (test and training features are exclusive). The classifier attempts to classify each signal into one of three bladder states: “Small”, “Medium” and “Full”. Bladder state classification results are presented for phantom Sets I and II, along with an analysis of misclassified signals.

4.1. Bladder State Classification Results

The number of PCA components is varied, 15 components were chosen to represent the best trade off between performance and computation as in [13], illustrated in Figure 4.

Overall mean bladder state accuracies and corresponding standard deviations are presented in Table 2. Bladder state classification performance for Set I phantoms is 91.33%, degrading slightly to 87.38% for the phantoms in Set II, while the standard deviation increases from 4.6% to 6.4% for mean results from Set I and Set II respectively. The increased muscle depth and larger bladder widths associated with

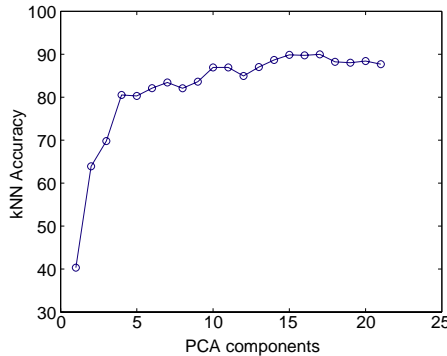


Figure 4. Plot of number of PCA components versus bladder state accuracy.

Table 2. Overall kNN classifier performances and corresponding standard deviations.

	Set I (%)	Set II (%)
Accuracy	91.33	87.38
σ	4.6	6.37

phantom Set II significantly attenuates the transmitted UWB pulse and resulting bladder reflections. However, even with the increase muscle and bladder depths of the phantom Set II, the performance of the classifier drops by less than 4%.

4.2. Misclassification Analysis

To adequately understand the behaviour of any classifier, it's important to analyse the misclassified signals. For the overall detection results, the percentage of each misclassified phantoms, specified by their associated bladder depths, are described in Tables 3 and 4. The fourth row of each table describes the incorrect bladder state corresponding to each misclassified phantom. For example, examining Table 3, one can see that the 10 mm bladder is only misclassified only 10.86% of the time. Of these 10 mm misclassifications, 80% of the time, the 10 mm was misclassified as a 20 mm bladder depth phantom and the remaining 20% correspond 30 mm bladder depth phantoms.

The most commonly misclassified phantoms from Set I are the 20 mm bladder depths (Medium), forming 58.69% of total misclassifications. These are mainly classified (86%) as 30 mm phantoms (Full) by the kNN algorithm. Similarly, 92% of the misclassified 30 mm bladder depths (Full) are incorrectly approximated as 20 mm phantoms (Medium) by the algorithm.

In Set II, the smallest bladder depth (20 mm) are the least misclassified, with a result of 18.04%. The percentage of Medium and Full bladder misclassifications are 37.11% and 44.84%, respectively. Similar to the Set I misclassifications, the two largest bladder depths

Table 3. Misclassification analysis of phantom Set I.

Width	Set I (%)		
	10 mm	20 mm	30 mm
Misclassified (%)	10.86	58.69	30.43
Misclassified as	20 mm (80%)	30 mm (86%)	20 mm (92%)

Table 4. Misclassification analysis of phantom Set II.

Width	Set II (%)		
	20 mm	30 mm	40 mm
Misclassified (%)	18.04	37.11	44.84
Misclassified as	30 mm (100%)	40 mm (68%)	30 mm (95%)

Table 5. Effect of sampling rate classifier performance.

Frequency (GHz)	Set I (%)	Set II (%)
50	91.33	87.38
30	90.82	87.60
15	93.12	83.23
10	77.71	73.76
5	56.92	48.82

are most commonly mistaken by the kNN algorithm as each other, where the 30 mm bladder depth phantoms are classified as 40 mm bladder depth phantoms, while the reverse is the case for misclassified 40 mm bladder depth phantoms.

Across both sets of phantoms, the smallest phantoms in each set are the best classified, where the reflection from the posterior bladder wall is strongest.

4.3. Effects of Sampling Frequency on Bladder State Classification

The development of any bladder state monitoring device would be subject to some cost/technological constraints. Therefore, the effects of different sampling rates should be considered. In order to examine this, the recorded signals are downsampled to various different sampling rates prior to any pre-processing and classification. The performance of the classifier at EACH sampling rate is shown in Table 5.

Classification results do not degrade significantly when the sampling frequency is reduced from 50 GHz to 15 GHz. At 30 GHz, results are similar to 50 GHz and while Set I accuracy actually improves at 15 GHz, the Set II detections deteriorate by just over 4%. Below 15 GHz, the classification performance drops significantly, degrading equally by 13.62% for both Set I and Set II. When signals are further downsampled to 5 GHz, the signal quality degrades significantly, and corresponding classification accuracies are significantly affected, dropping to 56.92% and 48.82%, for Set I and Set II respectively.

4.4. Antenna Aperture

As mentioned in the previous subsection, a bladder state monitoring device could be subject to some cost/technological constraints, including the number of antenna array elements. In this subsection,

Table 6. Effect of reduced antennas on kNN detection results.

Transmitters	Set I (%)	Set II (%)
4	91.33	87.38
3	79.43	71.31
2	85.48	79.92

the effects of reduced number of antenna array elements on the classification performance is considered.

To evaluate the performance of the bladder classification algorithm using three antennas, the signal data transmitted or received from one specific antenna element is removed from the dataset. To ensure a fair test, each antenna's contributions is removed in turn and four detection accuracies are recorded and the mean is presented in Table 6.

Using two antennas, the signal data from six separate combinations of TX-RX pairings are removed from the dataset in turn and the mean accuracies are given in row three of Table 6.

When a single antenna is removed, the mean accuracy is reduced to 79.43% for Set I and 71.31% for Set II. Results do not degrade significantly when two antennas are removed from the setup, with a decrease of over 5% and over 7% for Set I and Set II respectively.

5. CONCLUSIONS

This paper presents a UWB radar system to monitor the volume of urine present within the bladder. The system uses a k -nearest neighbour classification algorithm to classify the electromagnetic reflections from the bladder as corresponding to "Small", "Medium" or "Full". The prototype system is evaluated using dielectrically representative bladder phantoms, with varying muscle thicknesses and bladder sizes. The performance of the bladder state monitoring system exceeds 87%.

The performance of the system with respect to sampling rate and number of antenna array elements was also considered in this study. It was found that sampling rates greater than 10 GHz were required for classification performance greater than 70%. Finally, the performance of the classification algorithm was shown to be robust to the number of antenna array elements used. Even just using two antenna array elements, the average performance of the classifier was still more than 80%.

Overall, the prototype system presented in this paper illustrates the significant potential of UWB Radar based system for the

monitoring of bladder volume and significantly, the treatment of a wide range of urinary-related medical conditions. Future work will consider experimental scenarios where the antennas are located close to or on the skin, with the ultimate goal of developing a wearable bladder volume monitor.

ACKNOWLEDGMENT

The work was supported by Enterprise Ireland (grant number CF/2010/073) and Science Foundation Ireland (grant number 11/SIRG/I2120).

REFERENCES

1. Vulker, R., "International group seeks to dispel incontinence taboo," *Journal of the American Medical Association*, No. 11, 951–953, 1998.
2. Brown, J. S., E. Vittinghoff, J. F. Wyman, et al., "Urge urinary incontinence was associated with increased risk of falls and non-spinal, non-traumatic fractures in older women," *Evidence Based Nursing*, Vol. 4, No. 1, 26, 2001, [Online] Available: <http://ebn.bmj.com/content/4/1/26.short>.
3. Hu, T., T. Wagner, J. Bentkover, K. Leblanc, S. Zhou, and T. Hunt, "Costs of urinary incontinence and overactive bladder in the united states: A comparative study," *Urology*, Vol. 63, No. 3, 461–465, 2004.
4. Selius, B. and R. Subedi, "Costs of urinary incontinence and overactive bladder in the united states: A comparative study," *American Family Physician*, Vol. 77, No. 1, 443–450, 2008.
5. Crendon, M., "Primary nocturnal enuresis: Current concepts," *American Family Physician*, Vol. 59, No. 5, 1205–1214, 1999.
6. Petrican, P. and M. Sawan, "Design of a miniaturized ultrasonic bladder volume monitor and subsequent preliminary evaluation on 41 enuretic patients," *IEEE Transactions on Rehabilitation Engineering*, Vol. 6, No. 1, 66–74, Mar. 1998.
7. Niu, H., S. Yang, C. Liu, Y. Yan, L. Li, F. Ma, X. Wang, F. Pu, D. Li, and Y. Fan, "Design of an ultrasound bladder volume measurement and alarm system," (*iCBBE*) 2011 5th International Conference on Bioinformatics and Biomedical Engineering, 1–4, May 2011.
8. Li, X., E. Pancera, L. Zwirello, H. Wu, and T. Zwick, "Ultra

- wideband radar for water detection in the human body," *2010 German Microwave Conference*, 150–153, Mar. 2010.
9. Li, X., E. Pancera, L. Niestoruk, W. Stork, and T. Zwick, "Performance of an ultra wideband radar for detection of water accumulation in the human bladder," *2010 European Radar Conference (EuRAD)*, 212–215, Sep. 30–Oct. 1, 2010.
 10. Pancera, E., T. Zwick, and W. Wiesbeck, "Ultra wideband radar imaging: An approach to monitor the water accumulation in the human body," *2010 IEEE International Conference on Wireless Information Technology and Systems (ICWITS)*, 1–4, Aug. 28–Sep. 3, 2010.
 11. Geozondas, "Geozondas," 2012, [Online] Available: <http://www.geozondas.com/>.
 12. Wold, H., *Estimation of Principal Components and Related Models by Iterative Least Squares*, in *Multivariate Analysis*, K. Krishnaiah, Ed., Academic Press, New York, 1996.
 13. Conceicao, R. C., M. O'Halloran, M. Glavin, and E. Jones, "Support vector machines for the classification of early-stage breast cancer based on radar target signatures," *Progress In Electromagnetics Research B*, Vol. 23, 311–327, 2010.
 14. Cover, T. and P. Hart, "Nearest neighbor pattern classification," *IEEE Transactions on Information Theory*, Vol. 13, No. 1, 21–27, Jan. 1967, [Online] Available: <http://dx.doi.org/10.1109/TIT.1967.1053964>